FREQUENCY TUNED CO_2 LASER

R. L. Abrams

Hughes Research Laboratories

Prepared for:

Office of Naval Research
Advanced Research Projects Agency

March 1974

UNCLASSIFIED
Security Classification

AD 775656

DOCUMENT CONTROL DATA - R&D

(Security classification of title, body of abstract and indexing annotation must be entered when the overall report is classified)

1. ORIGINATING ACTIVITY *(Corporate author)*
Hughes Research Laboratories
3011 Malibu Canyon Road
Malibu, CA 90265

2a. REPORT SECURITY CLASSIFICATION
UNCLASSIFIED

2b. GROUP

3. REPORT TITLE

FREQUENCY TUNED CO_2 LASER

4. DESCRIPTIVE NOTES *(Type of report and inclusive dates)*
Interim Technical Report - 1 October 1973 through 31 December 1973

5. AUTHOR(S) *(First name, middle initial, last name)*
R. L. Abrams

6. REPORT DATE
March 1974

7a. TOTAL NO. OF PAGES
57

7b. NO. OF REFS
8

8a. CONTRACT OR GRANT NO.
N00014-73-C-0324

b. PROJECT, TASK, WORK UNIT NOS.
ARPA Order No. 1809

c. DOD ELEMENT

d. DOD SUBELEMENT

9a. ORIGINATOR'S REPORT NUMBER(S)

9b. OTHER REPORT NO(S) *(Any other numbers that may be assigned this report)*

10. DISTRIBUTION STATEMENT

11. SUPPLEMENTARY NOTES

12. SPONSORING MILITARY ACTIVITY
Advanced Research Projects Agency
Arlington, Virginia 22209

13. ABSTRACT

This program represents an effort to develop a stable, tunable CO_2 laser with a tuning range of ±750 MHz. In order to increase the tuning range of a CO_2 laser beyond the 50 to 100 MHz doppler broadening limited value, it is necessary to increase the gain linewidth. The technical approach taken here is to raise the operating laser pressure and thus broaden the gain linewidth. The linewidth broadens at the rate of 5.3 MHz/Torr and equals 1500 MHz at 283 Torr. High pressure operation is achieved by operating the laser in the waveguide mode, and thus using a small capillary bore as the gas discharge region.

In the first half of this program we have demonstrated a multiple electrode geometry which reduces discharge voltage requirements and improves laser discharge stability at high pressures. The successful use of an intracavity diffraction grating for line selection and an internally mounted bender bimorph for frequency tuning has been achieved. Laser tuning range data have been gathered under a variety of conditions on 1.5 mm i.d. and on 1.0 mm square BeO tubes incorporating the above features. The tuning range has been limited to ±600 MHz by fixed resonator losses (which include the grating, output mirror, and waveguide loss) and the bandwidth of laser transition at the operating pressure. The laser frequency stability has been measured to be better than 100 kHz, limited by mechanical resonances in the laser structure. An improved structure is being designed to eliminate this problem. The mechanisms for waveguide loss are studied in detail in this report, with the conclusion that they are not a major problem with present fabrication techniques.

DD FORM 1 NOV 65 1473

UNCLASSIFIED
Security Classification

14. KEY WORDS	LINK A		LINK B		LINK C	
	ROLE	WT	ROLE	WT	ROLE	WT
Waveguide Laser						
Tunable CO_2 Laser						
Tunable Local Oscillator						

HUGHES

HUGHES AIRCRAFT COMPANY
RESEARCH LABORATORIES

FREQUENCY TUNED CO_2 LASER

Interim Technical Report
Contract N00014-73-C-0324

Reporting Period: 19 March 1973 through 31 December 1973

ARPA Order No. 1806

Program Code No. 3E90

Effective Date of Contract: 19 March 1973

Contract Expiration Date: 30 June 1974

Amount of Contract: $135,224.00

Principal Investigator: R.L. Abrams
(213)456-6411

Scientific Officer: Director, Physics Programs
Physical Sciences Division
Office of Naval Research
Department of the Navy
800 North Quincy Street
Arlington, Virginia 22217

This research was supported by the Advanced Research Projects Agency of the Department of Defense and was monitored by ONR under Contract Nc. N00014-73-C-0324.

FOREWORD

The research reported here was accomplished with the advice and aid of the following people: H. R. Friedrich and R. E. Brower were primarily responsible for mechanical design and construction of the laser tubes, while M. B. Klein and G. Tangonan performed the analysis and experiments leading to an understanding of the mechanism for guide loss due to rough surfaces.

TABLE OF CONTENTS

LIST OF ILLUSTRATIONS

ABSTRACT

This program represents an effort to develop a stable, tunable CO_2 laser with a tuning range of ±750 MHz. In order to increase the tuning range of a CO_2 laser beyond the 50 to 100 MHz doppler broadening limited value, it is necessary to increase the gain linewidth. The technical approach taken here is to raise the operating laser pressure and thus broaden the gain linewidth. The linewidth broadens at the rate of 5.3 MHz/Torr and equals 1500 MHz at 283 Torr. High pressure operation is achieved by operating the laser in the waveguide mode, and thus using a small capillary bore as the gas discharge region.

In the first half of this program we have demonstrated a multiple electrode geometry which reduces discharge voltage requirements and improves laser discharge stability at high pressures. The successful use of an intracavity diffraction grating for line selection and an internally mounted bender bimorph for frequency tuning has been achieved. Laser tuning range data have been gathered under a variety of conditions on 1.5 mm i.d. and on 1.0 mm square BeO tubes incorporating the above features. The tuning range has been limited to ±600 MHz by fixed resonator losses (which include the grating, output mirror, and waveguide loss) and the bandwidth of laser transition at the operating pressure. The laser frequency stability has been measured to be better than 100 kHz, limited by mechanical resonances in the laser structure. An improved structure is being designed to eliminate this problem. The mechanisms for waveguide loss are studied in detail in this report, with the conclusion that they are not a major problem with present fabrication technqiues.

I. INTRODUCTION

Modern optical radar systems for surveillance of orbiting objects require a local oscillator for heterodyne reception which is capable of tracking changes in doppler shift. Present designs for a 10.6-μm imaging radar require a CO_2 laser local oscillator tunable ±750 MHz from line center. It is the purpose of this program to develop such a device.

Conventional CO_2 lasers are only tunable about ±50 MHz, limited by the gain linewidth. For conventional lasers, operating at 5 to 15 Torr, this linewidth is 50 to 100 MHz due to some pressure broadening in addition to the 53 MHz doppler width. In order to increase the tuning range, it is necessary to increase the gain linewidth. The technical approach taken here is to raise the operating laser pressure and thus pressure broaden the gain linewidth. The linewidth increases at a rate of ~5.3 MHz/Torr and equals 1500 MHz at a pressure of 283 Torr.

It has previously been demonstrated[1] at Hughes Research Laboratories that high pressure operation (above 300 Torr) of CO_2 lasers can be achieved under sealed-off conditions by operating the laser in the waveguide configuration. The discharge diameter of the laser is decreased as the pressure is increased, and increasing optical diffraction losses are avoided by using the narrow bore capillary as a hollow optical waveguide.[2]

In this program we have experimentally demonstrated a multiple electrode geometry which reduces discharge voltage requirements and improves discharge stability. We have demonstrated the use of intracavity diffraction gratings in waveguide lasers for wavelength selection and have designed and operated a bender bimorph holder for piezoelectric tuning of the laser. The bender bimorph and grating are all mounted inside the laser vacuum enclosure so that no Brewster windows are required in the device.

Laser tuning range data have been gathered under a variety of experimental conditions, both in 1.5 mm circular BeO tubes and in a 1.0 mm square BeO waveguide laser. A tuning range as high as ±600 MHz has been demonstrated, limited by fixed resonator losses which include the diffraction grating, mirrors, waveguide losses, and radiation leakage at the mirror waveguide interfaces. Each of these problems has been studied and the progress of these studies is included in this report.

In the following sections of this report we discuss the construction of the lasers used in these experiments, the sources of resonator losses and their limitations on tuning range, and our experimental work to date. Considerable attention has been given to the problem of how surface properties of the waveguide effect guiding loss; this problem is discussed in detail here.

II. TECHNICAL PROGRESS

Technical progress has been made on a number of different problems relating to the design of a tunable, high pressure, waveguide CO_2 laser. These include electrode geometry; waveguide fabrication, including a study of waveguide loss; mounting of optical elements; choice of optics; and mounting of a piezoelectric mirror translator internal to the vacuum enclosure. In this section we discuss the progress made to date in these areas.

A. Preliminary Experiments

Two crucial experiments were performed early in the program to prove out concepts which we proposed for the tunable laser. These related to electrode geometry and the use of a diffraction grating for line selection.

The proposed electrode geometry is similar to that shown in Fig. 1. The advantage of such a configuration is that both ends of the laser can be at ground potential (although this is not shown in Fig. 1), which simplifies the electrical circuitry for the bender bimorph and also has a safety advantage. Operation with negative high voltage allows the cathodes (center electrodes) to be removed from the optics, avoiding problems with sputtering damage to the mirrors.

In order to test the above concept, the test section shown in Fig. 1 was fabricated. The tube consists of a BeO bore, 8.5 cm x 1.0 mm i.d., and the electrodes are hollow nickel pins. It was found that all four discharge paths could be simultaneously excited at pressures up to 300 Torr. When the high voltage was increased slowly, some paths would not light, but when turned up suddenly, all paths usually light simultaneously. At pressures above 200 Torr, however, several attempts were necessary in order to light all paths. It should be a simple matter to start all paths together with either a Tesla coil or a high voltage pulse for a final power supply design.

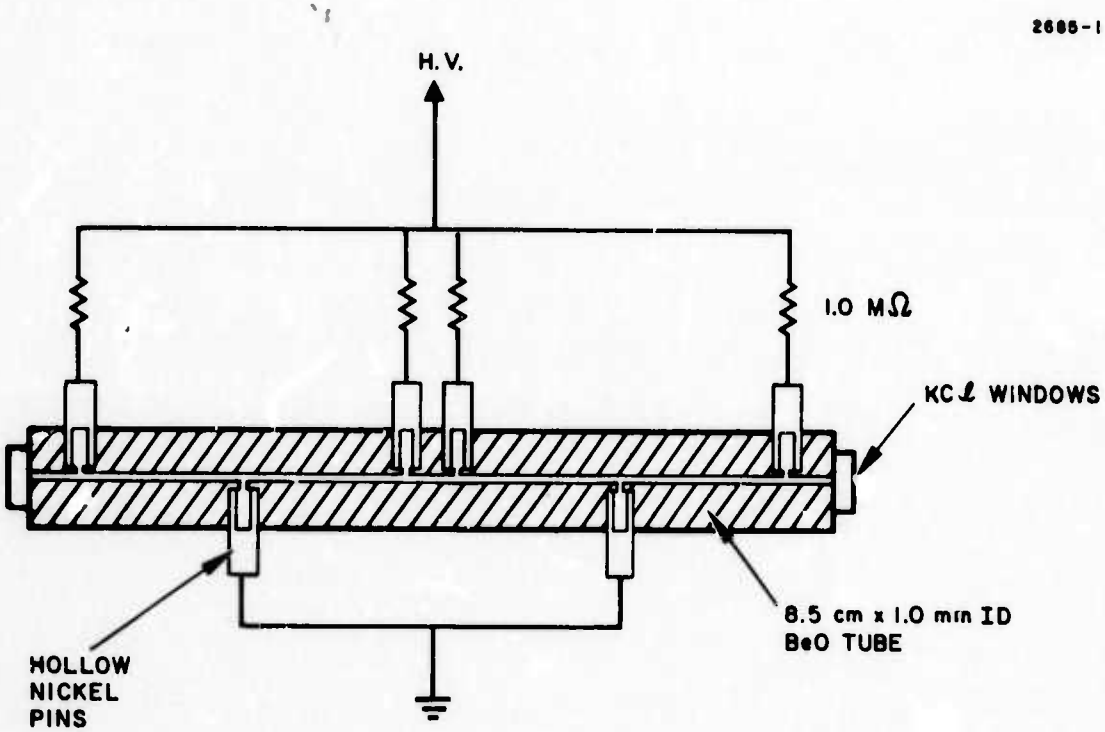

Fig. 1. Test section for multiple electrode geometry.

The use of a diffraction grating in a waveguide laser places some severe requirements on the grating. It must possess a Littrow diffraction efficiency high enough (above 95%) to be used in these low gain lasers and must be capable of withstanding very high power densities (>1 kW/cm^2). Our past experience has shown that some replica gratings have efficiencies greater than 95% when overcoated with gold, but damage occurred when used as reflectors in conventional lasers. We have found, however, that if the replica is mounted on copper, rather than glass, the increased thermal conductance prevents damage. For this reason, we acquired a Bausch and Lomb #35-53-04-890, 150 ℓ/mm, 8/μm blaze grating mounted on a copper substrate.

Careful measurements of Littrow reflectivity for this grating at 10.6 μm showed a reflectance of 97% for the polarization normal to the grating grooves and 20.5% for the polarization parallel to the grooves. Thus, when used as a reflector, the grating acts as a polarization selector as well as a line selector. The energy reflected specularly for the 97% Littrow orientation was less than 1%, so more than 2% of the energy is dissipated or scattered.

We found that if these gratings were covered with a commercial strippable protective covering, they could be cut with a cutting wheel and the reflectivity was unchanged after the coating was removed. In this manner, a number of gratings usable for waveguide lasers were obtained from a single purchased grating.

An adjustable mount was fabricated to test one of the cut pieces in a 1.5 mm square x 10 cm Al_2O_3 waveguide CO_2 laser. The laser produced ~0.6 W on P(20) of the $00^0$1 to 10^0) transition, about half the power expected with a total reflector replacing the grating. This is consistent with the fact that the 3% loss from the grating is close to the 4% loss on the output mirror.

We were able to select a number of transitions with this fixture. No damage was observed on the diffraction grating after operation for several hours. The only difficulty was that, as the laser thermally tuned over one free spectral range, a higher order transverse mode

The use of a diff action grating in a waveguide laser places some severe requirements on the grating. It must possess a Littrow diffraction efficiency high enough (above 95%) to be used in these low gain lasers and must be capable of withstanding very high power densities (>1 kW/cm^2). Our past experience has shown that some replica gratings have efficiencies greater than 95% when overcoated with gold, but damage occurred when used as reflectors in conventional lasers. We have found, however, that if the replica is mounted on copper, rather than glass, the increased thermal conductance prevents damage. For this reason, we acquired a Bausch and Lomb #35-53-04-890, 150 ℓ/mm, 8/μm blaze grating mounted on a copper substrate.

Careful measurements of Littrow reflectivity for this grating at 10.6 μm showed a reflectance of 97% for the polarization normal to the grating grooves and 20.5% for the polarization parallel to the grooves. Thus, when used as a reflector, the grating acts as a polarization selector as well as a line selector. The energy reflected specularly for the 97% Littrow orientation was less than 1%, so more than 2% of the energy is dissipated or scattered.

We found that if these gratings were covered with a commercial strippable protective covering, they could be cut with a cutting wheel and the reflectivity was unchanged after the coating was removed. In this manner, a number of gratings usable for waveguide lasers were obtained from a single purchased grating.

An adjustable mount was fabricated to test one of the cut pieces in a 1.5 mm square x 10 cm Al_2O_3 waveguide CO_2 laser. The laser produced ~0.6 W on P(20) of the $00^0 1$ to 10^0) transition, about half the power expected with a total reflector replacing the grating. This is consistent with the fact that the 3% loss from the grating is close to the 4% loss on the output mirror.

We were able to select a number of transitions with this fixture. No damage was observed on the diffraction grating after operation for several hours. The only difficulty was that, as the laser thermally tuned over one free spectral range, a higher order transverse mode

operation was observed. These various modes were often on rotational lines adjacent to the centrally tuned line, and were occasionally separated by two lines. The operating pressure for these experiments was ~150 Torr. At this pressure the laser gain linewidth (~800 MHz) is less than a free spectral range (~1200 MHz).

The results of this experiment show that the diffraction grating is a suitable optical element for waveguide lasers. Although the diffraction efficiency (97%) achieved is impressive, it is clear that the goals of this program would be better served if a grating with higher efficiency were available. An attempt to fabricate such a grating is being made here at Hughes Research Laboratories.

In a preliminary experiment, Dr. H. L. Garvin showed that it was possible to ion machine sawtooth-shaped grooves in germanium and other materials. In an attempt to make a blazed grating, a 12-μm line spacing was machined in a ZnS coated glass blank. After overcoating with gold, this grating had a measured Littrow efficiency of 95%. Even more impressive was the fact that no energy was measured in zero order (<0.1%), so considerable energy was lost to absorption and scatter. Since the ZnS was polycrystalline, it is believed that a higher quality grating can be machined in a single crystal surface. Such a grating will be fabricated in germanium. In addition to the potentially high efficiency, these gratings should be capable of handling large power densities, as they will have no replicating layer to act as thermal isolation for the reflecting surface.

With the successful completion of the above preliminary experiments, the fabrication of two lasers for tunable local oscillator experiments was initiated.

B. Laser Fabrication

The construction of the 1.5 mm i.d. circular bore laser is discussed with reference to Fig. 2. The body of the laser consists of a 1 in. o.d. x 9.5-cm long BeO rod. A 1.5-mm diameter hole is drilled the length of the rod and counterbored holes are provided from the sides

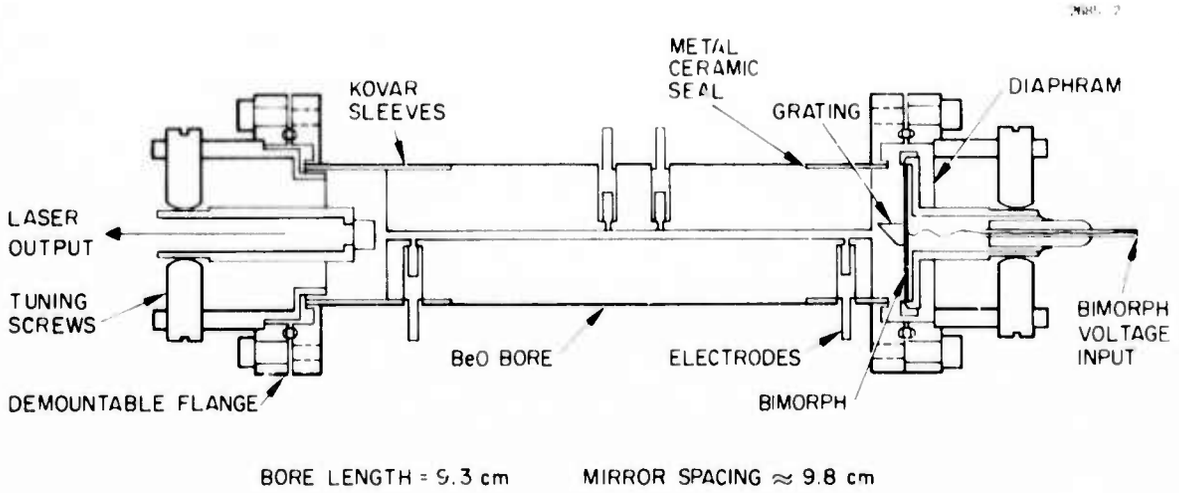

Fig. 2. Construction details of tunable laser.

for electrodes as shown. Kovar sleeves are brazed to the BeO ends which have been metallized. Copper gasketed vacuum flanges are welded to these sleeves and all subsequent hardware is mounted by means of mating flanges.

The 1.0-mm square bore lasers are fabricated from polished BeO slabs, 9.5-cm long, epoxied together to form a 1.0-mm square waveguide. In this case, the copper gasketed flanges are machined to fit over the rectangular outer dimensions of the tube, and are epoxy sealed. A photograph of the pieces used to fabricate these tubes is shown in Fig. 3.

Special flange mounted mirror alignment devices have been designed and built for these tubes. The mirror holder and the bender bimorph device are mounted on a post which is brazed through a 0.010-in. stainless steel diaphragm. Adjustments of the mirror or grating alignment are made by turning the adjusting screws and flexing the diaphragm. The grating and mirror are epoxied to their respective holders and the bender bimorph is held against a nylon retaining ring by a threaded holder. The electrical connection to the bimorph is made through a ceramic feedthrough through the end of the adjustment device.

The bender bimorph is a one inch circular disc, 0.020 in. thick and is composed of two oppositely poled piezoelectric discs, bonded together. Application of a voltage across the bimorph causes the 1-in. disc to buckle slightly, resulting in a linear motion at the center of the disc, normal to its plane. The bimorph holder serves to clamp the disc at its edge and provides for electrical connection.

A 2.0 mm x 10 cm waveguide laser was fitted with a totally reflecting mirror mounted on the bimorph and a 96% reflecting output mirror. A linear ramp voltage was applied to the bimorph, and the ramp as well as laser output is displayed in Fig. 4. The ramp height is 210 V and 9 orders (or half wavelengths) are displayed. Thus, the average sensitivity of the bimorph is 0.28 μ/V and about 23 V are required to tune the laser over one order (5.3 μm).

M10138

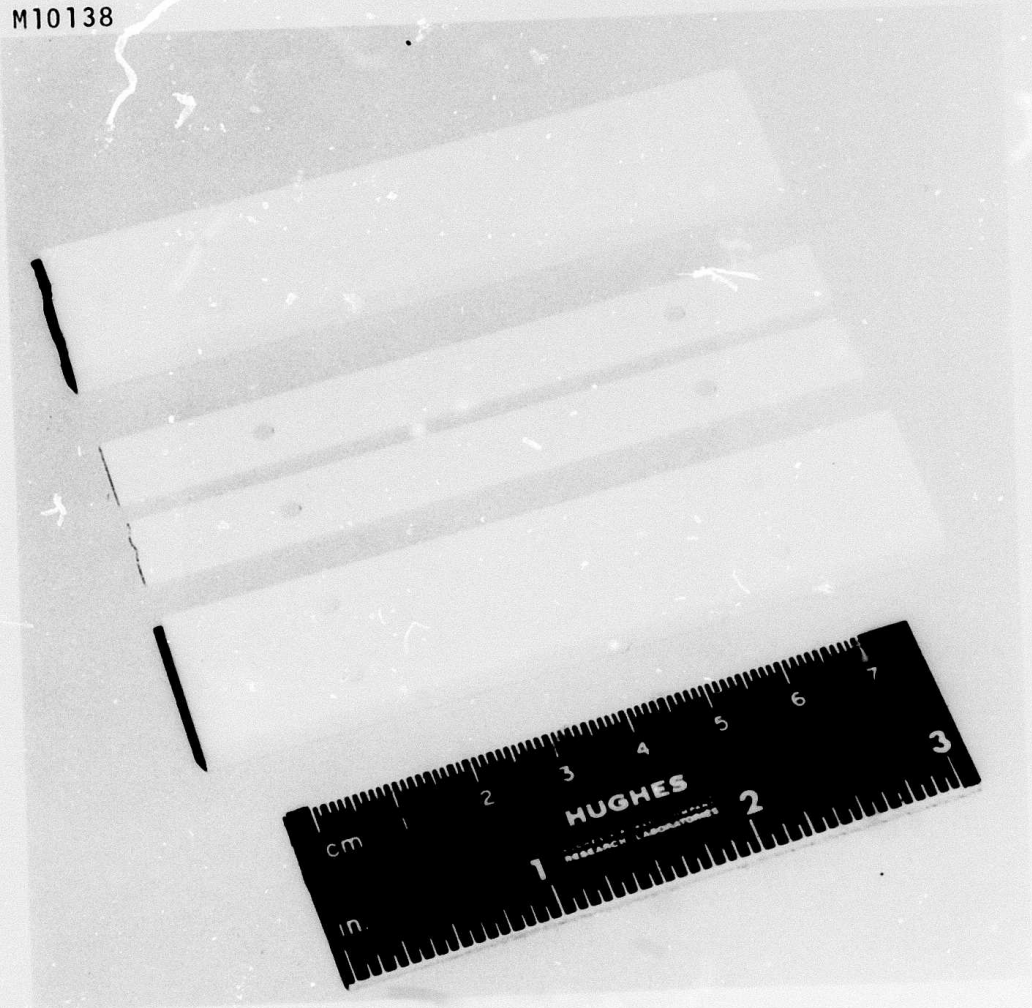

Fig. 3. Pieces used to fabricate 1.0 mm square bore tube.

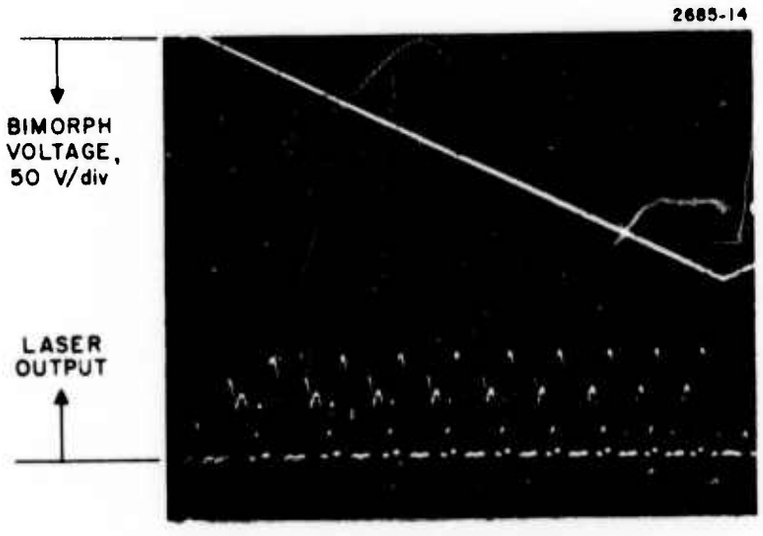

Fig. 4. Laser output and bimorph voltage.

The electrodes consist of hollow nickel pins epoxied into the countersunk holes. The 1.5-mm circular bore laser is mounted into an aluminum heat sink as shown in the photograph in Fig. 5(a). Evacuation and gas fill are provided by the feedthrough in one of the flanges as shown. The aluminum heat sink is cooled by flowing water. The 1.0-mm square bore laser is shown mounted on its heat sink in Fig. 5(b).

The laser and related hardware form a rugged and stable package. This concept of a single, monolithic structure with internally mounted mirrors should result in excellent laser frequency stability.

C. Tuning Experiments – 1.5 mm Circular Bore Tube

Measurements of tuning range for these lasers have been made by observing the signature of the laser output as a linear ramp voltage is applied to the bender bimorph. This also provides a convenient technique for testing the bender bimorphs. The experimental arrangement for tuning range measurements is shown in Fig. 6. The output of the tunable laser is monitored with a monochromator and detected with a dc-coupled photoconductor. A linear ramp voltage generator drives the bender bimorph. The output of the laser versus bimorph voltage can be displayed either on an oscilloscope (fast scan) or on an X-Y recorder (slow scan). Both techniques have been employed in these experiments.

The bender bimorphs have the capability of scanning over several half-wavelengths at 10.6 μm, allowing the display of a number of free spectral ranges in the laser tuning characteristic. One free spectral range corresponds to 1530 MHz of tuning for our 9.8 cm laser cavities. This serves as a calibration for measuring the frequency range over which a single line may be tuned.

The two 1.5 mm circular bore tubes built for this program have been designated A-17 and A-18, respectively. Prior to installation of diffraction gratings in these tubes, simple output power measurements were made using a 96% reflecting output coupling mirror (3% transmission) and a total reflector. Tube A-18 gave 1.1 W output while

M9864

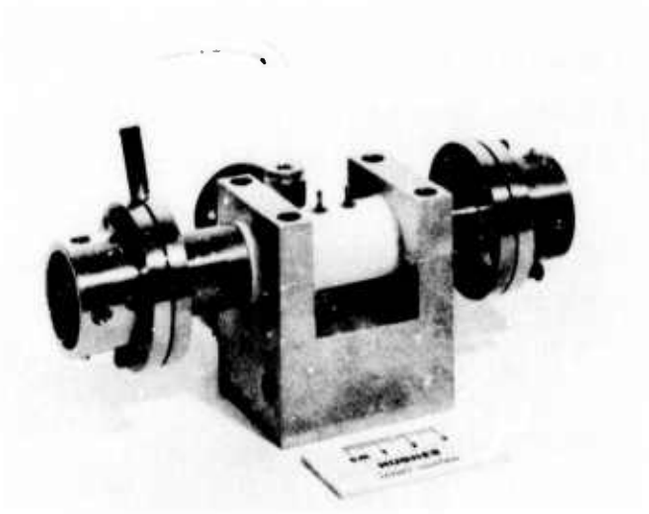

(a)

M10137

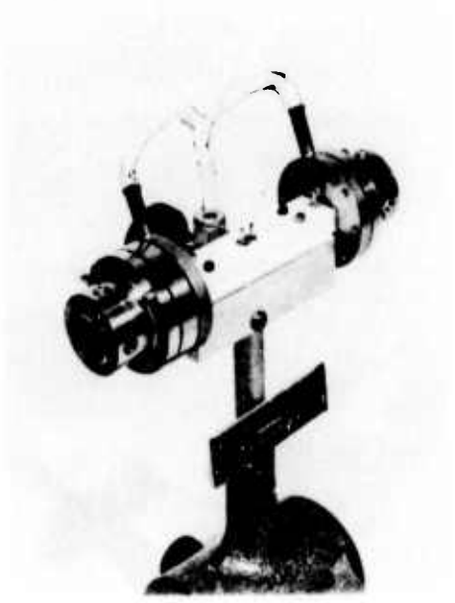

(b)

Fig. 5. Tunable laser with (a) i.d. circular bore and (b) 1.0 mm square bore.

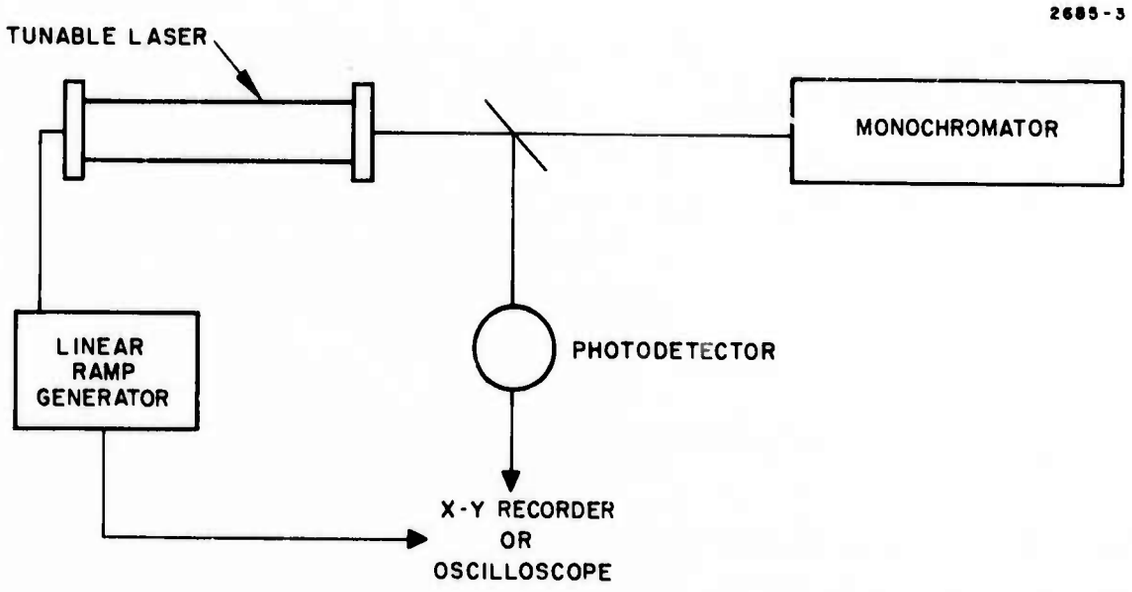

Fig. 6. Experimental arrangement for tuning range measurements.

A-17 gave only 0.9 W. The rest of the results reported on here were made on the better laser tube. Later measurements in our inspection shop showed that the tube which gave more output power also had a straighter bore. Bore straightness is an important quality in determining waveguide loss as discussed in the section on waveguide losses.

Measurements of the laser signature, and thus tuning range, were made under a variety of conditions. The largest tuning range, when power was extracted from the 96% reflecting output coupler, occurred at a pressure of 140 Torr with a $He:CO_2:N_2:Xe$ mixture of 4:1:0.5:0.25. Under these conditions, tube voltage and current were 4.1 kV and 2.0 mA through each side. The laser signature for this case is shown in Fig. 7. The peak laser output power is 0.65 W and the laser tuning range is 776 MHz. The tuning range over which the power level exceeds half the peak value (3 dB tuning range) is 674 MHz. Note that three lines lase over different parts of the laser tuning curve, but the highest power transition, P(20), is lasing alone over its tuning curve. This fact was confirmed by observation with the spectrometer.

After some aging of the tube and minor readjustment of the mirror and grating alignment, the data of Fig. 8 were taken. Here we used the X-Y recorder to record the data. Only two lines were lasing except at the lowest pressure (100 Torr) where a third line lased for a small region of the tuning curve. The maximum tuning range occurred at 140 Torr, and equalled 653 MHz.

Degnan[3] has shown that the tuning range for a homogeneously broadened laser is given by

$$2\left|\nu_c - \nu_o\right| = \Delta\nu\left[\frac{g_o L}{\ell n\left(1/\sqrt{r_1 r_2}\right)} - 1\right]^{1/2}$$

where $|\nu_c - \nu_o|$ is the tuning range from line center, $\Delta\nu$ is the full linewidth at half maximum, g_o is the small signal laser gain coefficient at line center, L is the active laser length, and r_1 and r_2 are the

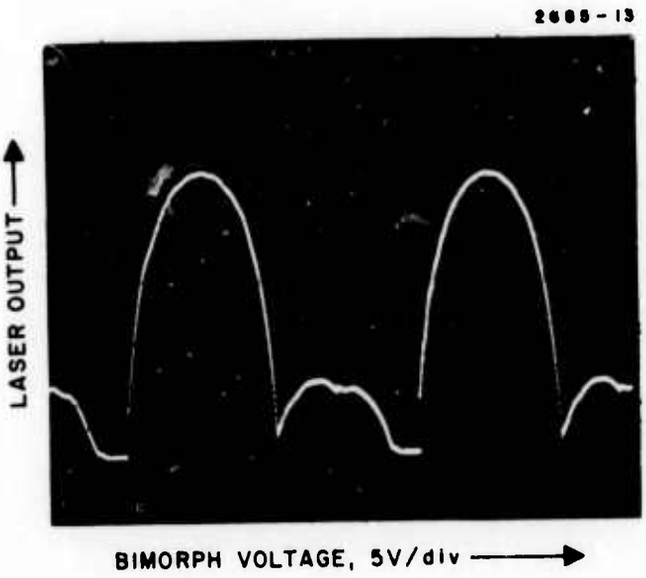

Fig. 7. Laser output power versus bimorph tuning for tube A-18.

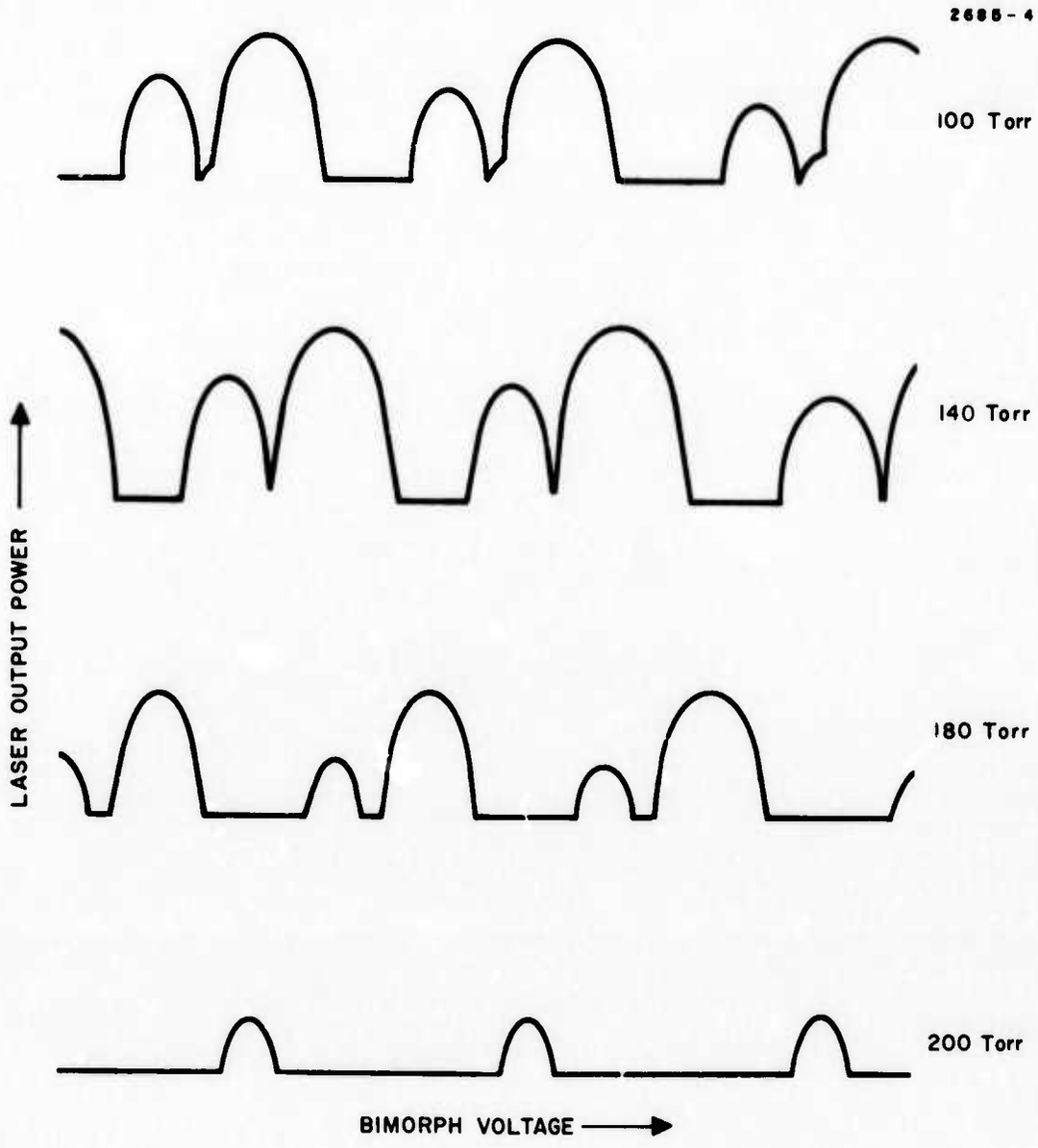

Fig. 8. Tuning characteristic of tube A-18 for various total gas pressures.

reflectivities of the two mirrors. In our case n = 0.96, r_2 = 0.97, g_o = 0.01 cm^{-1} (see Ref. 1), L = 8.3 cm and at 140 Torr $\Delta\nu$ = 742 MHz. Thus, we find for the calculated value,

$$2\left|\nu_c - \nu_o\right| = 855 \text{ MHz.}$$

We can consider this excellent agreement with experiment. Assume that there is an additional round trip loss r_3 which reduces the tuning range according to

$$2\left|\nu_c - \nu_o\right| = \Delta\nu\left[\frac{g_o L}{\ell n\left(1/\sqrt{r_1 r_2 r_3}\right)} - 1\right]^{1/2}$$

Then for the values quoted above, and with the experimental value $2\left|\nu_c - \nu_o\right|$ = 776 MHz,

$$r_3 = 0.992.$$

Thus, the additional loss required to explain the reduction in expected tuning range at 140 Torr is only 0.8% round trip or 0.4% single pass. As we shall see from our waveguide loss measurements, we have observed waveguide transmission in excess of 99%, consistent with these results. It is clear from the above results that decreasing the waveguide diameter and reduction of losses in the optical components will be important to the success of this program.

D. Tuning Experiments – 1.0 mm Square Bore Tube

The 1.0 mm square waveguide laser, denoted tube A-20, was first fitted with a flat output mirror (96% reflecting, 3% transmission) and a flat total reflector, mounted on a bimorph. Output power was then measured as a function of gas mixture and total pressure. The results are shown in Fig. 9. The significance of this data is that the

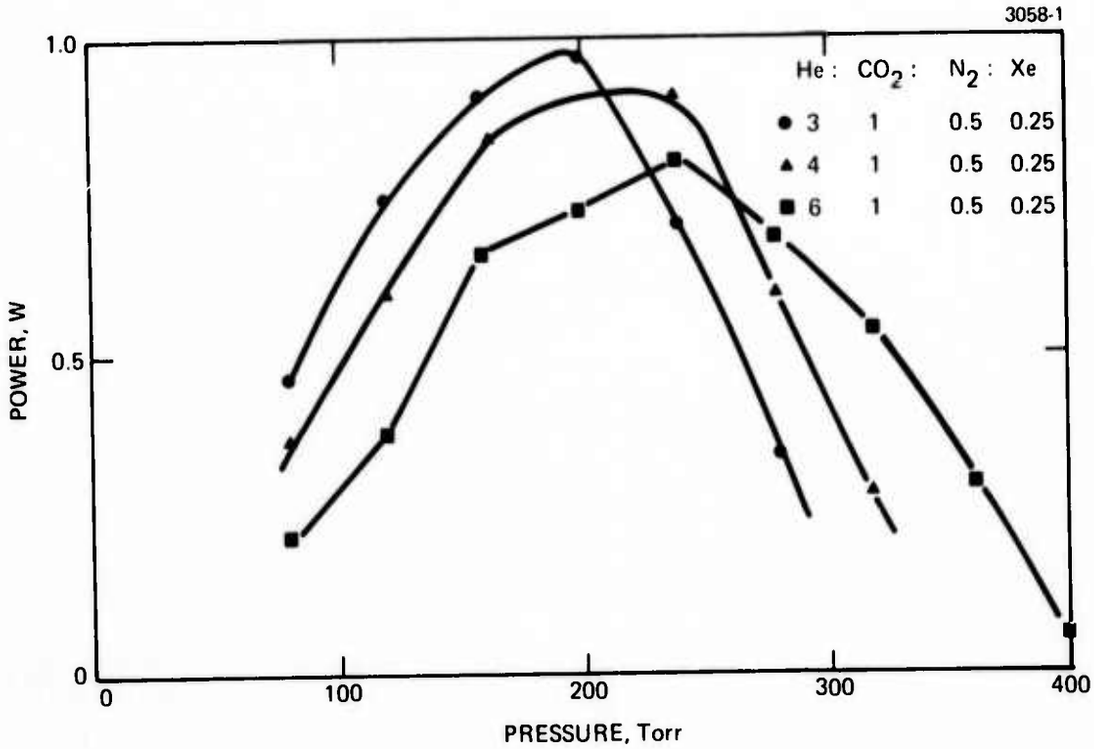

Fig. 9. Output power versus gas pressure for tube A-20.

available power from the 1.0-mm tube is about the same as obtained from the 1.5-mm circular bore tube of the same length (A-19) and the optimum pressure is in the 200 to 300 Torr region rather than 150 Torr as found for the A-18. We should expect a correspondingly larger tuning range.

The total reflector was replaced with a diffraction grating and tuning curves were obtained in the same manner as for A-18. Representative data are shown in Fig. 10 for an 8:1:0.5:0.25 mixture of $He:CO_2:N_2:Xe$. The maximum tuning range observed here is ~930 MHz. The tuning range and output power are plotted versus pressure in Fig. 11 for a different gas mix (4:1:0.5:0.25). It is seen that the maximum tuning range and maximum power both occur at approximately the same pressure (~200 Torr for this mixture), as predicted by the theory of Degnan.[3] The maximum output power is ~0.5 W.

The output mirror was then replaced with a total reflector and the output power is coupled off of the zeroth order of the grating. This coupling was rather small, resulting in only 80 mW of laser power at the P(20) line center, but allowing us to measure the tuning range. Representative data for the 8:1:0.5:0.25 mixture are shown in Fig. 12. The maximum tuning range was observed to be 1200 MHz at a total pressure of 260 Torr. The tube voltage and current are 6.6 kV and 1.5 mA through each side. We have found that the tuning range increases for lower tube current, probably due to decreased gas heating (higher density) and higher gain, even though laser output power is lower at lower current.

E. Frequency Stability

Tubes A-17 and A-18 (1.5 mm circular bore tubes) were fitted with diffraction grating and output mirrors, and heterodyned together in a HgCdTe photoconductor. Both tubes were mounted on an aluminum block which was supported on polyurethane foam in a normal laboratory environment. The tube bases were water cooled and the laser power supplies had less than 5 mV peak-to-peak ripple. The IF output from

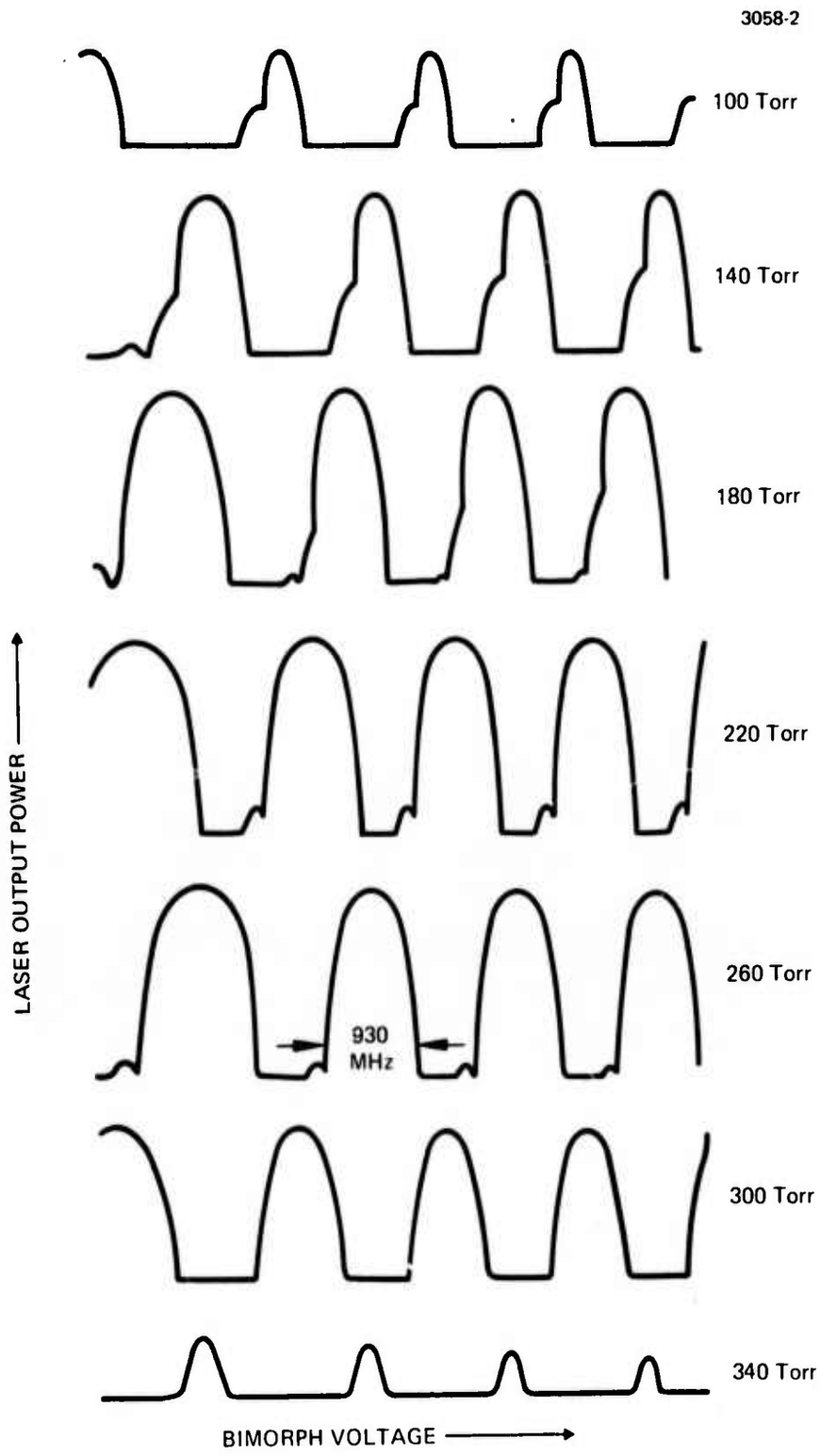

Fig. 10. Tuning characteristic of tube A-20, with power taken through output mirror, for various total gas pressures.

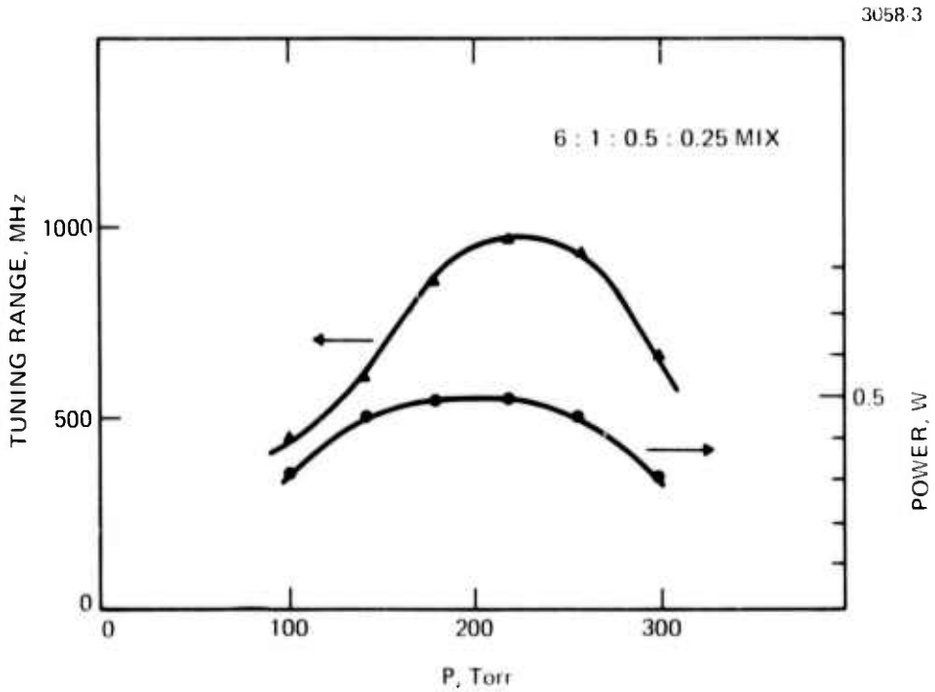

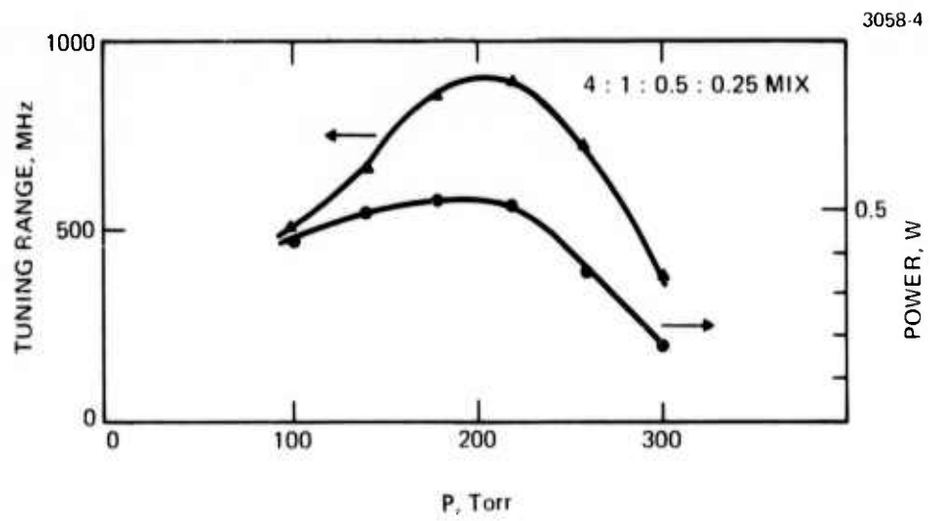

Fig. 11. Observed tuning range and output power versus pressure for tube A-20.

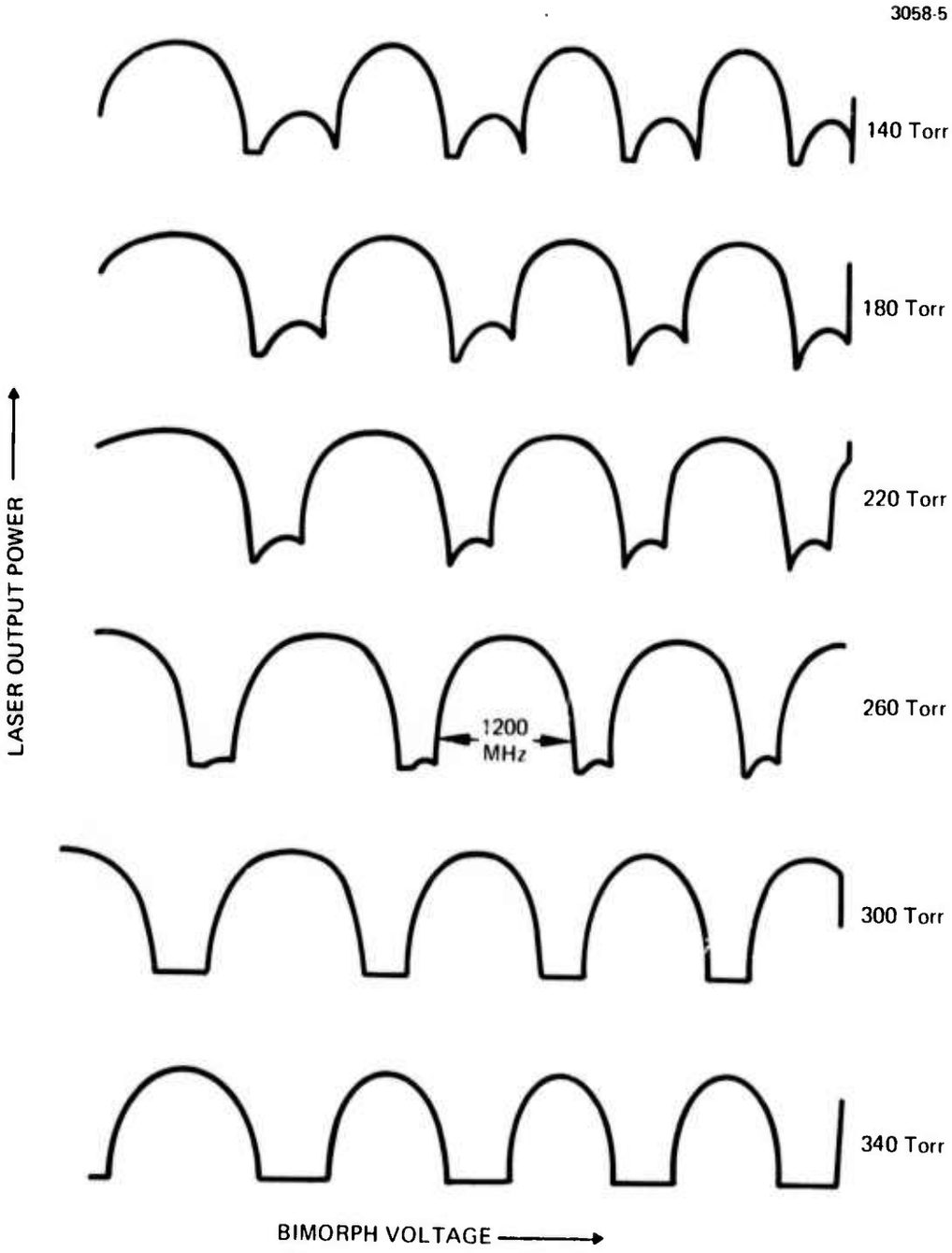

Fig. 12. Tuning characteristic of tube A-20, with power coupled off of grating, for various total gas pressures.

the detector was displayed on a spectrum analyzer and also passed through a 30 MHz discriminator and displayed on an oscilloscope. In this manner, the frequency deviations could be directly observed in real time, independent of long term drift.

Typical spectrum analyzer displays are shown in Fig. 13. For these pictures, the IF bandwidth was 10 kHz, the scan rate was 3 ms/cm, and the center i. f. frequency was 80 MHz. The spectrum analyzer was used in the log mode with a vertical sensitivity of 10 dB/cm.

It is clear from these displays that the frequency stability falls short of the program goal of 1 kHz (short term). Looking at the real time output of the discriminator reveals some of the source of this instability.

Figure 14(a) shows the discriminator output with the cooling water flowing through the tube base. The peak frequency deviations are ~0. 2 MHz and are nearly sinosoidal at a frequency of ~2. 3 kHz. Turning the cooling water off momentarily results in the output shown in Fig. 14(b). The peak variations in frequency are now ~60 kHz, but still have the strong ringing at 2. 3 kHz.

The mechanical structure of the laser and bimorph apparently have a strong resonance at 2. 3 kHz, which swamps out any other perturbations of the laser frequency. The end structures are being redesigned to eliminate the steel diaphram and to raise the resonant frequency of the bimorph. Additional isolation of the tube from the laboratory environment will also improve the frequency stability.

F. Waveguide Losses

In order to insure efficient operation of a waveguide gas laser, it is essential to keep guiding losses as small as possible. For a waveguide bore with a smooth, straight interior surface, the losses are due only to leakage into the guiding medium from the bore. For the lowest order EH_{11} mode the loss coefficient may be written as[2]

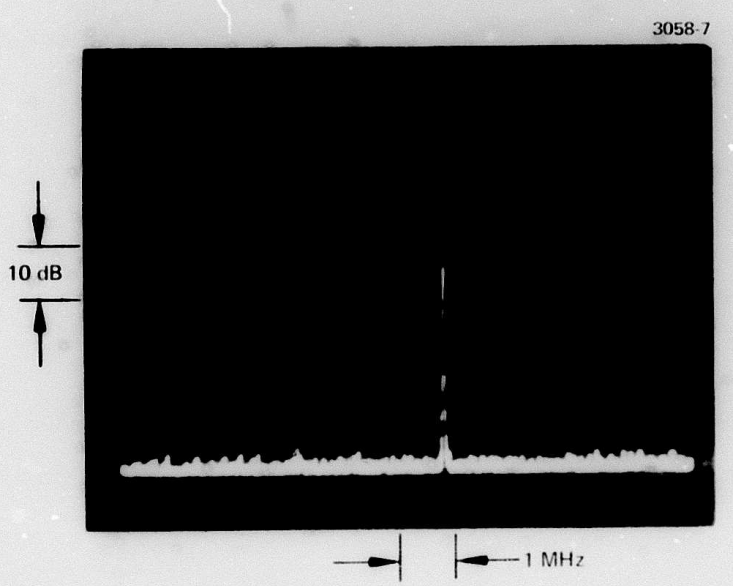

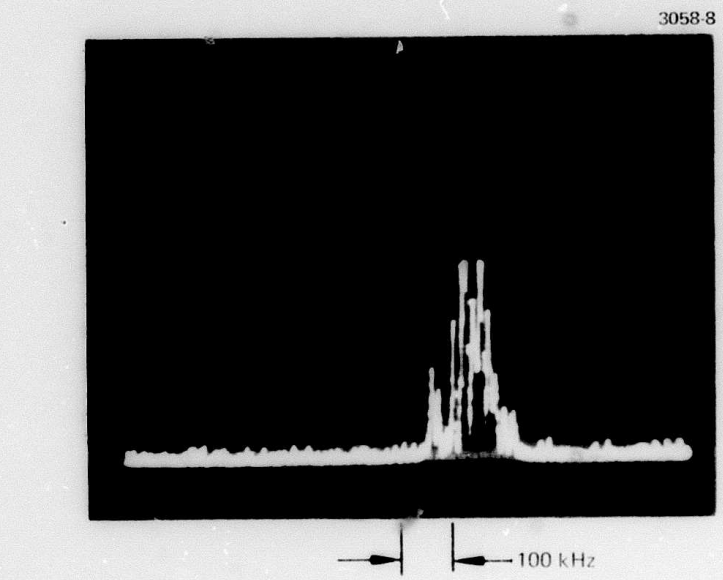

Fig. 13. Spectrum analyzer displays of best frequency between tubes A-17 and A-18.

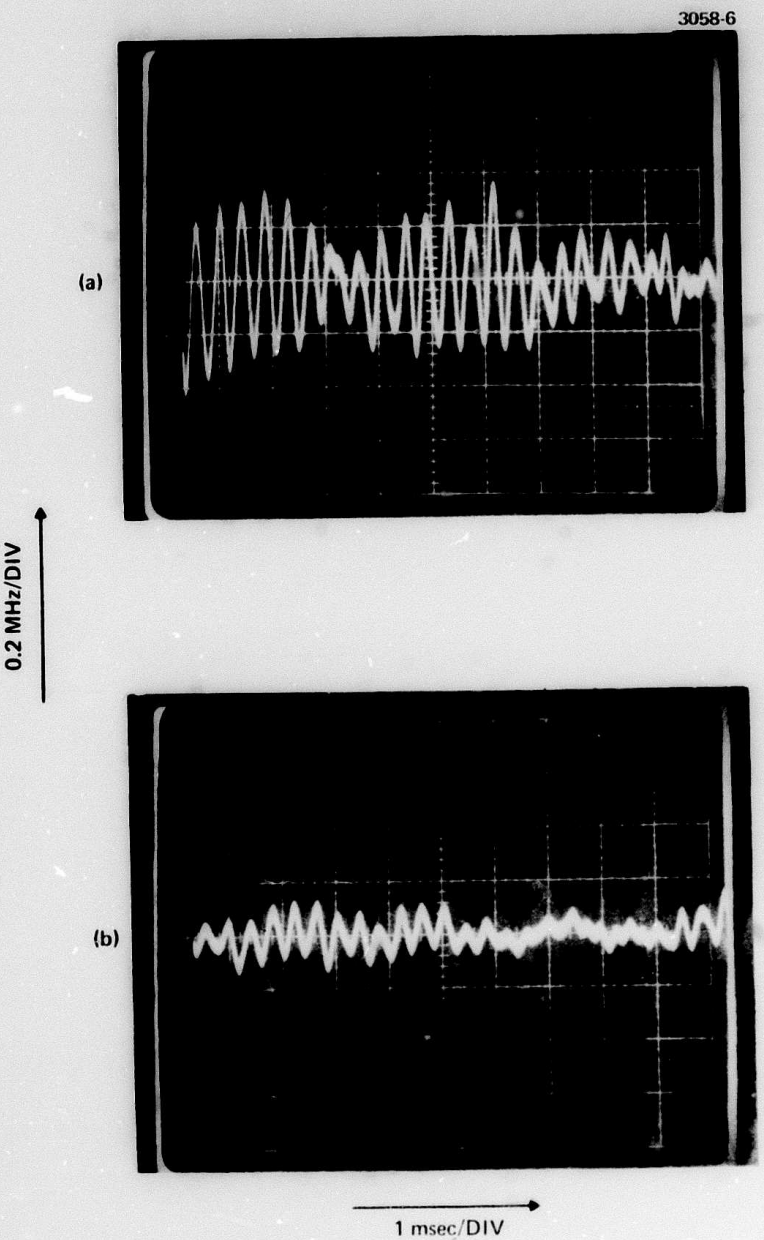

Fig. 14. Output of frequency discriminator with 30 MHz i.f. input from mixing of two waveguide lasers, A-17 and A-18. Top trace is for water flow on, and bottom trace shows the output with water flow off.

$$\alpha_{11} = \left(\frac{2.405}{2\pi}\right)^2 \frac{8\lambda^3}{D^3} \mathrm{Re}(\nu_n),$$

where D is the bore diameter and ν_n is an expression involving the complex index of refraction of the wall material $\nu = n\text{-}ik$,

$$\nu_n = \frac{1/2\left(\nu^2+1\right)}{\left(\nu^2-1\right)^{1/2}}$$

Thus, for a given bore radius and wavelength, the best bore material is one whose optical constants yield the smallest value[1] of $\mathrm{Re}(\nu_n)$. Of all the potential bore materials, the one with the smallest value of $\mathrm{Re}(\nu_n)$ at 10.6 μ is BeO. For this material we find $\alpha_{11} = 4.3 \times 10^{-5}$ cm^{-1} for a 1-mm diameter waveguide at 10.6 μ; other potential bore materials such as alumina, quartz or pyrex all yield loss coefficients on the order of 2×10^{-3} cm^{-1}.

As mentioned earlier, there are two effects which can produce an increase in waveguide loss over the ideal case as given in eq. (1). The first is a lack of straightness of the waveguide bore. Marcatili and Schmeltzer[2] have shown that for a waveguide with uniform bend radius R, the loss coefficient for the EH_{11} mode is given by

$$\alpha(R) = \alpha(\infty)\left\{1 + 4/3\left(\frac{2\pi a}{2.405\,\lambda}\right)^4 \cdot \left(\frac{a}{R}\right)^2\left[1 + \frac{1}{(2.405)^2} + \frac{3}{4}\,\frac{\mathrm{Re}\left(\sqrt{\nu^2-1}\right)}{\mathrm{Re}\left(\frac{\nu^2+1}{\sqrt{\nu^2-1}}\right)}\cos 2\theta_o\right]\right\}$$

Here $\alpha_{11}(\infty)$ is the loss coefficient for a straight guide, a is the bore radius, and θ_o is the angle between the mode polarization and the plane of bending. For example, a 60 m radius bend in a 1.5 mm BeO waveguide increases the straight guide loss by 17 to 41%, depending on the polarization orientation.

A second potential contribution to the waveguide loss arises from the departure from ideal smoothness of the interior bore surface. It is expected that a rough surface will scatter more light out of the specular direction than a smooth surface, thereby lowering the waveguide transmission. The strength and functional dependence of this effect are considered in detail in subsequent sections.

1. Effects of Surface Roughness on Specular Reflectivity

The propagation of a guided mode through a waveguide laser bore may be considered to proceed via a series of grazing incidence specular reflections from the interior wall surface. If one can predict the intensity loss for each wall reflection, then the loss of each mode can be obtained from the angle of incidence and number of reflections. A convenient expression for specular reflectivity as a function of roughness and angle also permits a convenient optical measurement of the surface roughness of flat samples.

The most comprehensive theory relating reflectivity to surface roughness is given by Beckmann.[4] In this treatment the surface is considered to possess a statistical distribution of surface heights w(z), where w(z) is the probability of measuring a height z above the plane z = 0, and is characterized by a correlation distance T, which is a measure of the roughness density on a horizontal scale.

By applying diffraction theory in the Kirchhoff approximation, Beckmann obtains an expression for the amplitude reflectivity ρ of a rough surface in the specular direction:

$$\rho = \int_{-\infty}^{\infty} w(z)\, e^{ik_z z}\, dz \,. \qquad (1)$$

In this expression we have

$$k_z = \frac{4\pi}{\lambda} \cos \theta, \qquad (2)$$

where θ is the angle of incidence. It may be seen from Eq. (1) that the amplitude reflectivity is just the Fourier transform of the surface height distribution function.

The intensity reflectivity is related to the amplitude reflectivity by

$$R = \langle \rho\rho^* \rangle . \tag{3}$$

The reflectivity as given here is applicable to rough metal surfaces, where the reflectivity in the absence of roughness is unity. In the case of a rough dielectric surface, the above expression is modified in a straightforward way to yield

$$\frac{R}{R_o} = \langle \rho\rho^* \rangle \tag{4}$$

where R_o is the reflectivity of a smooth surface of the same material. In cases where the optical constants of the bulk material are known, R_o may be calculated directly from the Fresnel equations.

For a given surface height distribution w(z), the above relations may be used to derive an expression for the reflectivity ratio R/R_o as a function of θ, λ and σ. One commonly encountered distribution is the so-called normal (gaussian) distribution given by

$$w(z) = \frac{1}{\sigma\sqrt{2\pi}} e^{-z^2/2\sigma^2} \tag{5}$$

By substitution into eqs. (1) and (4), we obtain

$$\frac{R}{R_o} = e^{-\left(\frac{4\pi\sigma\cos\theta}{\lambda}\right)^2} . \tag{6}$$

We may also consider a Lorentzian distribution for w(z), given by

$$w(z) = \frac{\sigma}{\pi} \frac{1}{\sigma^2 + z^2} . \tag{7}$$

In this case we find

$$\frac{R}{R_o} = e^{-\frac{8\pi\sigma}{\lambda} \cos\theta} . \tag{8}$$

It may be seen from eqs. (6) and (8) that for $\sigma \cos\theta \to 0$, we obtain $<\rho\rho^*> \; 1$. This result is, in fact, valid for any (normalized) distribution w(z) as seen from eq. (1) with $k_z = 0$, and may be derived independently of any restrictions on σ or T. This is a very powerful result since even for rough surfaces ($\sigma \approx \lambda$), the specular reflectivity still approaches unity at grazing incidence. Experimental results to be described later support this conclusion.

2. Effects of Surface Roughness on Waveguide Loss

In this section we derive expressions which will be used to discuss the effect of wall roughness on losses in one-dimensional waveguides, in line with Beckmann's theory[4] of the modification of the specular reflection for rough surfaces. We first derive approximate formulae for the TM and TE reflectivities r^o_{TM} and r^o_{TE} of a smooth surface at glancing incidence. The rough surface reflectivities for TM and TE polarizations are obtained by multiplication of the Beckmann factor, so that

$$r_{TE,\,TM} = r_{TE,\,TM}\, e^{-\left(\frac{4\pi\sigma \sin\phi}{\lambda}\right)^2}$$

where ϕ is the glancing angle, and we have assumed a gaussian surface height distribution.

Fresnel's equation for a medium of indices (n_1, k_1) give for the reflectivities r^o_{TM} and r^o_{TE}:

$$r^o_{TM} = \frac{(n_1 \sin\phi - 1)^2 + k_1^2 \sin^2\phi}{(n_1 \sin\phi + 1)^2 + k_1^2 \sin^2\phi}$$

$$r^o_{TE} = \frac{(n_1 \sin\phi - 1)^2 + k_1^2 \sin^2\phi}{(n_1 + \sin\phi)^2 + k_1^2}$$

For small ϕ, and using the condition $n_1 \gg k_1$, we derive approximations for r^o_{TM} and r^o_{TE}:

$$r^o_{TM} \doteq 1 - 4n_1\phi$$

$$r^o_{TE} \doteq 1 - \frac{4n_1\phi}{n_1^2 + k_1^2}$$

The Beckmann modification of r^o_{TM} and r^o_{TE} for a normally distributed rough surface is thus

$$r_{TM} = (1 - 4n_1\phi)\, e^{-\left(\frac{4\pi\sigma\phi}{\lambda}\right)^2}$$

$$r_{TE} = \left(1 - \frac{4n_1\phi}{n_1^2 + k_1^2}\right) e^{-\left(\frac{4\pi\sigma\phi}{\lambda}\right)^2}$$

We now derive an expression for the waveguide losses in terms of wall reflectivity, waveguide thickness, and grazing angle ϕ. For the path shown in Fig. 15, the intensity in the guide is diminished by $1 - r^2$ over the path length $2a \cot\phi$, so for the low loss TE and TM modes,

$$\alpha_{TE,\,TM} = (1 - r^2_{TE,\,TM})/2a \cot\phi \,.$$

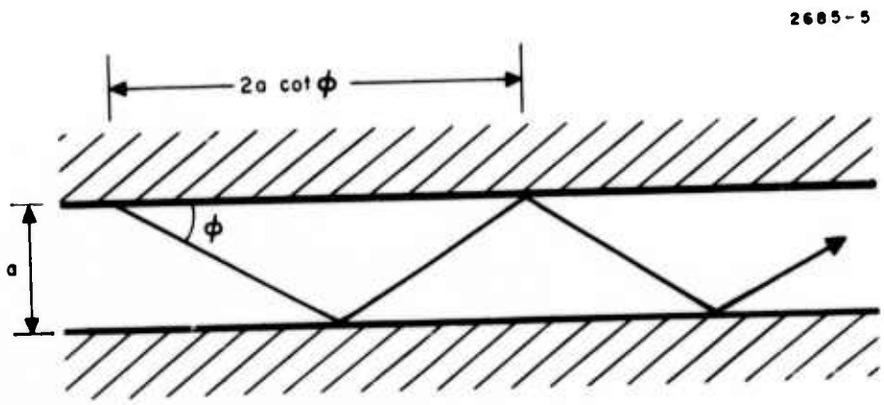

Fig. 15. Ray optics view of planar waveguide mode.

The angle ϕ is determined from the phase condition

$$\left[\frac{2\pi}{\lambda} \sin \phi\right] a = 2\pi(\nu+1)$$

where ν is the mode index. Therefore, for small ϕ

$$\cot \phi = \frac{a}{(\nu+1)} .$$

For the case of small σ, simplifications in the expressions for absorption may be made with the result

$$\alpha_{TM} = \frac{(\nu+1)^2 \lambda^2 n_1}{a^3} \exp\left[2(4\pi\sigma\phi/\lambda)^2\right] = \alpha^o_{TM} \exp\left[2(4\pi\sigma\phi/\lambda)^2\right]$$

$$\alpha_{TE} = \frac{(\nu+1)^2 \lambda^2 n_1}{a^3 (n_1^2 + k_1^2)} \exp\left[2(4\pi\sigma\phi/\lambda)^2\right] = \alpha^o_{TE} \exp\left[2(4\pi\sigma\phi/\lambda)^2\right],$$

As a check with the more conventional derivation of Marcuse we present Marcuse's approximation for α^o_{TE} of a smooth planar guide:

$$\alpha^o_{TE} = \frac{(\nu+1)^2 \lambda^2}{a^3 \sqrt{n^2-1}}$$

Both approaches yield quite similar results when we put $\sigma = 0$ (smooth guides), but our results are directly applicable to discussions of the effects of wall roughness on laser performance, when viewed according to Beckmann's theory.

3. Experimental Results for Waveguide Loss

In this section we will describe several experiments intended to determine the influence of interior wall surface quality on the transmission of typical laser bores. Included in these experiments are studies of flat ceramic surfaces, loss measurements in one-dimensional glass waveguide structures of known surface quality, and

loss measurements in circular pyrex, quartz, and BeO laser waveguides. Besides providing useful information on the importance of wall scattering, the results of this section also help to identify other types of imperfections leading to increased guiding losses.

a. Studies of Flat Ceramic Surfaces – In order to characterize and specify the quality of the interior walls of waveguide laser structures, we have performed extensive studies of polished and unpolished flat ceramic surfaces of alumina and beryllium oxide. We have made use of three techniques for studying these surfaces: scanning electron microscope (SEM) photographs, mechanical surface profile measurements, and optical reflectivity measurements.

The ceramics used in laser structures are manufactured by mixing fine particles of the material with a binder and then compressing and/or firing the sample to remove the binder. This process also fuses the material and promotes grain growth; typical grain sizes are in the range of 1 to 5 μ. The uniformity and quality of the ceramic are determined largely by the compression and firing. If those processes are not accomplished satisfactorily, the material will contain pores which will limit the quality of a polished surface. Furthermore, the average grain size of the material is a significant parameter, since it determines the lateral roughness scale of the ceramic surface.

Figure 16 is an SEM photograph of a flat BeO surface comparable in quality to that encountered on the interior of our laser structures. Our laser bores are produced by a grinding operation using a thin drill; the sample surface shown here has been machined flat from the same material. The surface structure here is quite chaotic, with a scale of variation comparable to the expected grain size. In order to determine the vertical roughness a scale of this same sample, we have mechanically examined its surface using a Dektak surface profile machine with a 30-μ diameter stylus; a typical scan is shown in Fig. 17. We see here that the surface possesses peak-to-peak excursions of approximately 5 μ, with an rms value of approximately 1 μ.

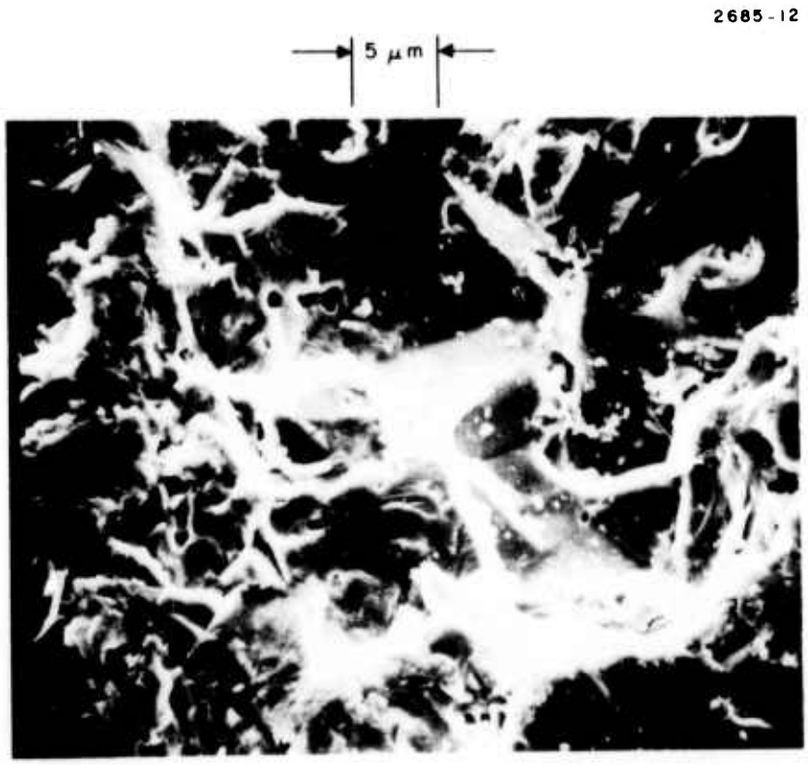

Fig. 16. SEM photograph of machined beryllia surface.

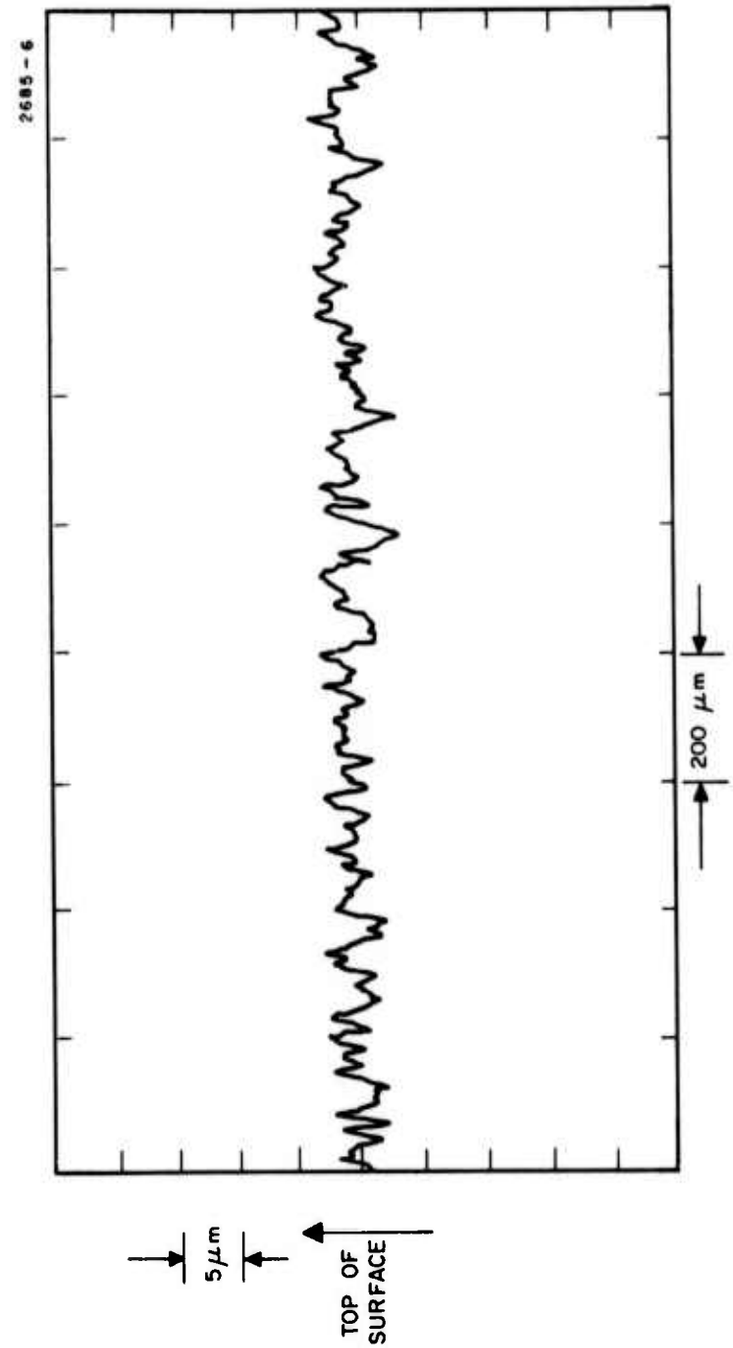

Fig. 17. Surface profile scan of machined beryllia surface.

By comparison with the previously measured sample, we show in Fig. 18 an SEM photograph (at the same magnification as Fig. 15) of an alumina surface which has been polished in our optical shop; a corresponding Dektak scan is shown in Fig. 19. This surface is nearly free of pores and has been polished to an rms flatness of approximately 30 Å. We have found that the BeO samples studied tend to be relatively porous, thus limiting the finish of a polished surface to approximately 200 Å.

Another important technique for examining rough surfaces is the study of optical specular reflectivity. Previously, expressions were obtained for the reflectivity ratio R/R_o as functions of σ, λ and θ for two common surface height distributions. Other distributions yield different functional dependences but they all yield unity reflectivity as $\sigma \cos\theta/\lambda$ approaches 0. The most convenient way to verify this dependence is to measure the specular reflectivity R as a function of angle, and plot the logarithm of the reflectivity ratio R/R_o versus $\cos^2\theta$ (assuming a gaussian distribution) or $\cos\theta$ (assuming a Lorentzian distribution). If a straight line is obtained in either case, then the slope may be related directly to the roughness σ. Even if some other distribution is applicable, a plot of reflectivity versus $\cos\theta$ (or $\cos^2\theta$) should extrapolate to 1 for $\cos\theta = 0$.

Typical results for two samples are shown in Fig. 20. Sample A is the same BeO surface studied earlier (see Figs. 16 and 17), and sample B is a second BeO surface with a crude polish. The results are plotted versus $\cos\theta$, since sample B fits a straight line very well in this case. If we assume sample B to be characterized by a Lorentzian distribution of surface heights, we obtain (from the slope) the value of σ shown. In the case of sample A, the indicated value of σ was obtained from the average slope and is in good agreement with this Dektak value. In both cases the curves extrapolate very close to unity at $\cos\theta = 0$ (grazing incidents), in spite of the minimal polish which the surfaces possess.

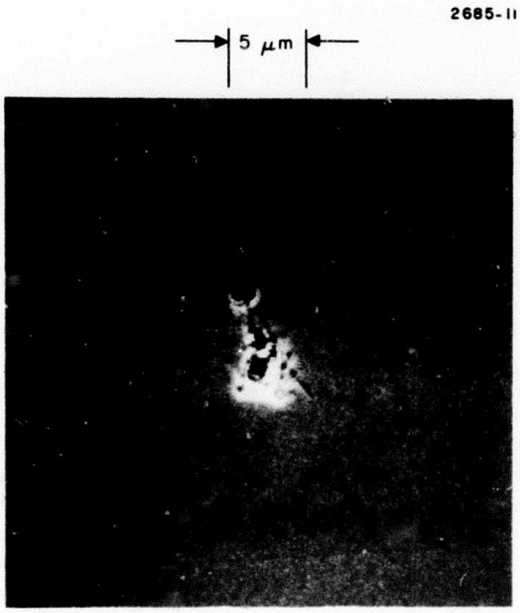

Fig. 18. SEM photograph of polished alumina surface.

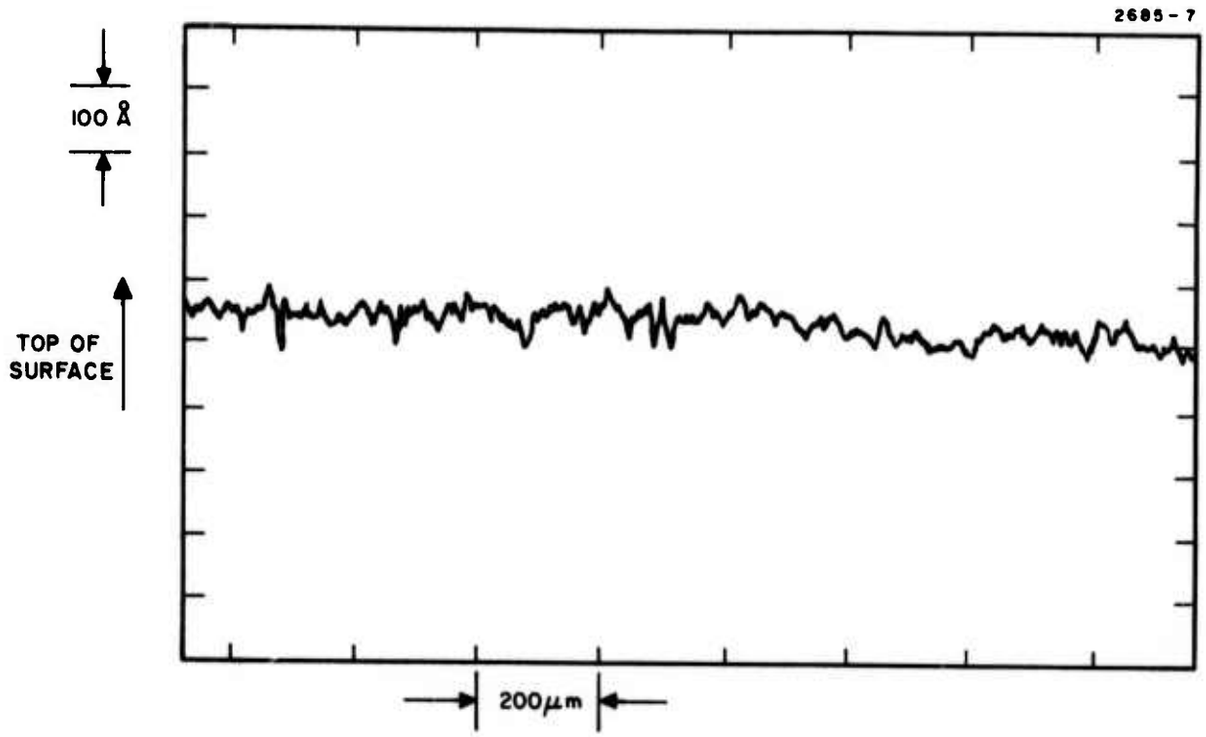

Fig. 19. Surface profile scan of polished alumina sample.

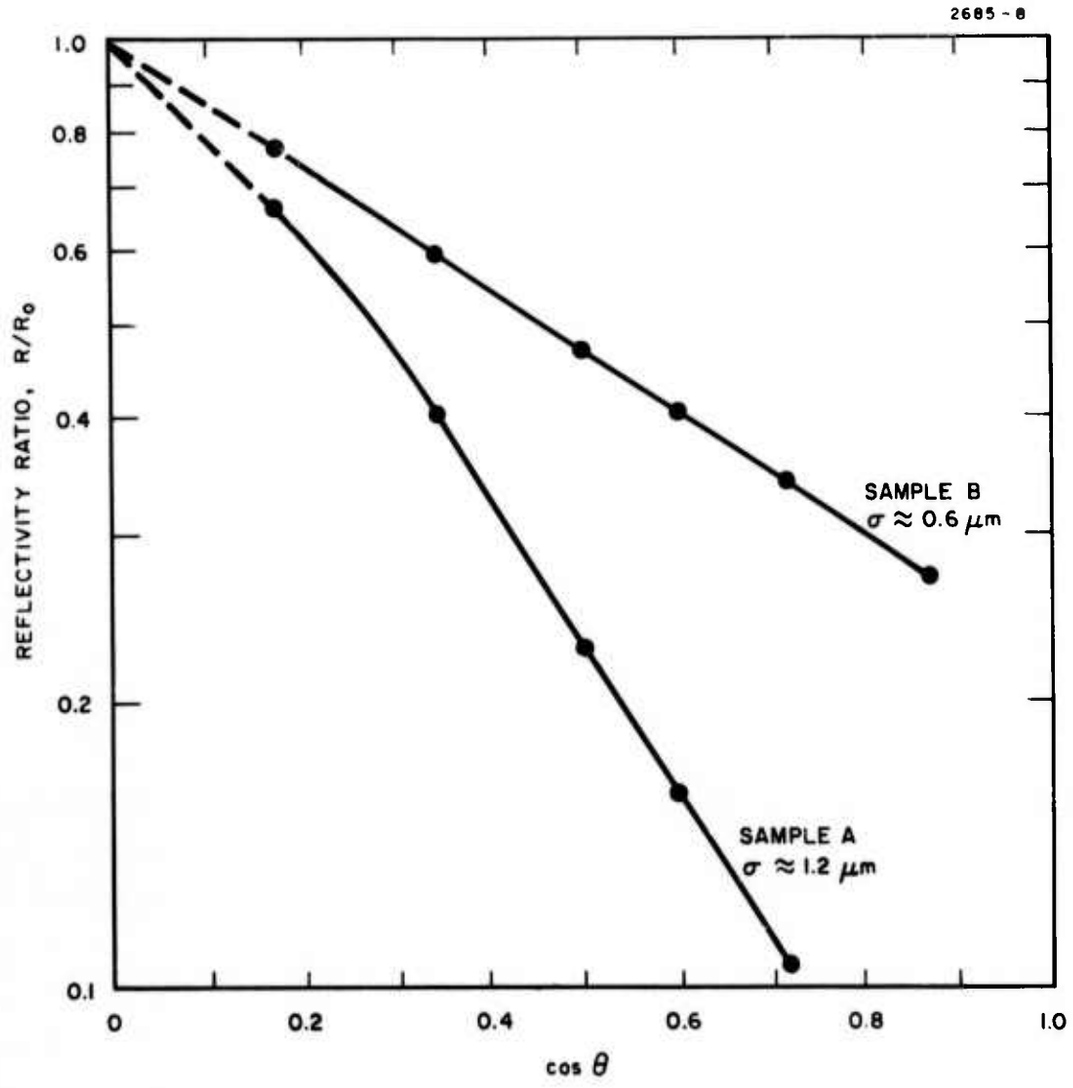

Fig. 20. Reflectivity ratio R/R_0 versus cos θ.

It is important to note that the smooth surface reflectivity $R_o = R_o(\theta)$ used in the above analysis has been obtained by substitution of measured optical constants[5] of single crystal BeO (at 10.6 μ) into the Fresnel equations. We had hoped to perform an independent measurement of those constants for our ceramic samples by measuring $R(\theta)$ on highly polished surfaces, for which $R \approx R_o$; in this case the optical constants n and k could be determined (using the Fresnel equations) from reflectivity measurements at two different angles. Unfortunately, we were unable to obtain surfaces of sufficient smoothness to make meaningful measurement. However, our best surfaces provide apparent optical constants in close enough agreement with single crystal values to justify using the latter; this practice is also common in previous literature.[6]

b. Circular Waveguide Loss Measurements – Waveguide transmission measurements were made of actual waveguide laser structures of BeO and of quartz and pyrex waveguides of various diameters (1 mm, 0.8 mm, and 0.5 mm). We will first describe the experimental procedures employed and then summarize our results.

While the actual transmission measurements are straightforward, special care was given to the aligning of the samples with respect to the input beam and the matching of the CO_2 laser beam waist to the sample diameter to afford optimum coupling to the lowest order EH_{11} mode. A Lansing mirror mount was adapted to accommodate the laser tubes. This apparatus, when placed on a vertical-horizontal translator, served well to position and align the samples with respect to the laser input beam. As evidence of the necessity to position and align the tubes carefully, Fig. 21 shows two photographs of the far-field pattern as observed on thermographic paper when only slight misalignment occurs. The far-field pattern for a well aligned sample is shown for the sake of comparison. In all the experimental results we report, the input beam radius at its waist was adjusted to 0.6435 a, where a is the tube radius. This optimum matching condition was

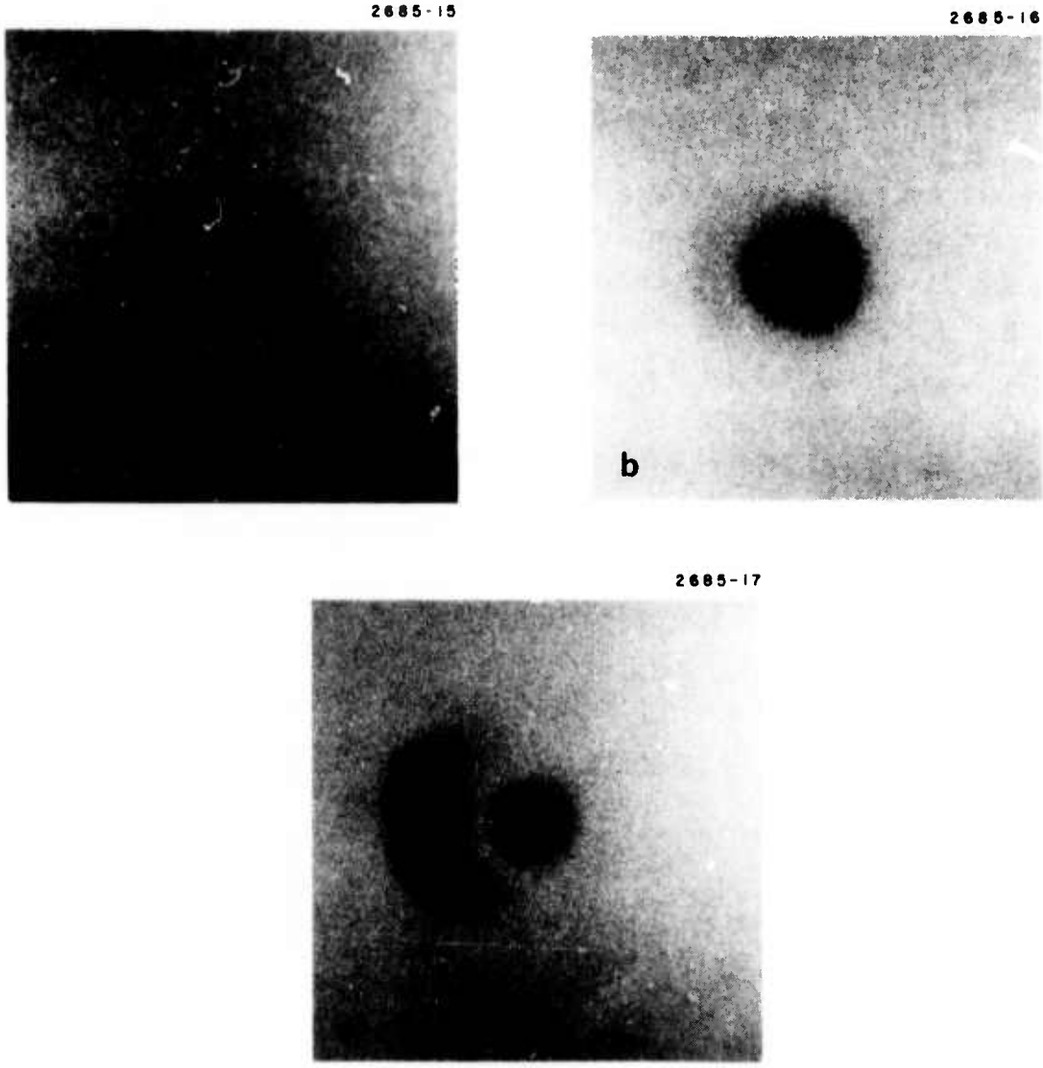

Fig. 21. Far field radiation patterns for (a) null aligned, (b) slightly misaligned, and (c) misaligned waveguide.

previously derived by Abrams.[7] For such a beam, 98% of the input beam is coupled to the EH_{11} mode and 99.3% of the total power is coupled into the waveguide. Throughout our experiments a 2 W single mode CO_2 laser which had been stabilized to within 1% variation was used.

Waveguide transmission measurements were performed on quartz and pyrex precision bore tubing obtained from Wilmad Glass Company. The tubes for which measurements were made were of 0.4, 0.5, 0.8, 1.0 mm in diameter and 15.5 cm in length. The bore tolerances quoted by the manufacturer are ±0.005 mm. No special effort was made to assure extremely straight tubes.

The transmission was measured first for the original length and later for smaller lengths obtained by carefully breaking the tubes. From the plots of transmission versus length and using the known coupling factor to the EH_{11} mode, the waveguide losses for this mode are calculated. These measurements are summarized for waveguides of quartz and pyrex of various diameters in Fig. 22.

Two conclusions can be made based on these results:

1. The theoretically predicted d^{-3} behavior of the waveguide losses is directly verified by our measurements.

2. The absolute magnitude of the measured losses is higher by approximately four times for both quartz and pyrex than the values predicted by theory. The degree of straightness of these tubes must influence this result greatly.

The second conclusion is supported in the following way. From reflectivity measurements we have experimentally verified the value of $Re(\nu_n)$ for pyrex and the result $Re(\nu_n) = 1.43$ agrees well with the values used in calculating the theoretical loss. Since we have ensured optimum coupling to EH_{11} the increased losses are not due to higher order modes. Finally, a calculation was performed to determine the radius of curvature which could affect such an increase. The radii required are in the range of 25 m, where a 100-m radius indicates

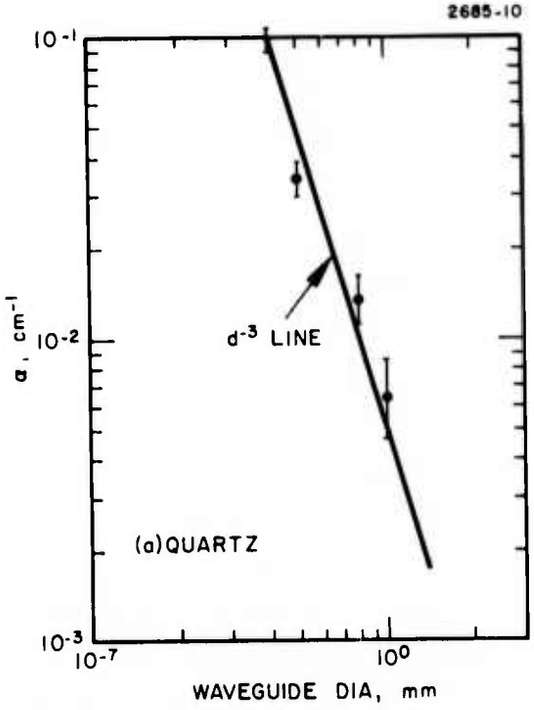

(a) Quartz.

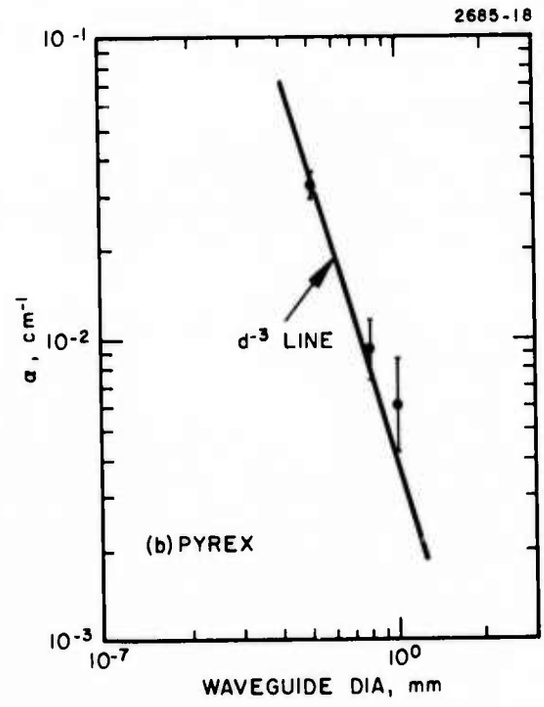

(b) Pyrex tubing.

Fig. 22. Measured waveguide losses for precision bore.

straightness to within 0.1 mm in 10 cm. Curvatures in this range are certainly not unreasonable for the tubes, which are obtained as precision bore tubes with only nominal straightness requirements.

Waveguide transmission measurements were also performed on actual laser structures of 1-mm bore BeO tubes. Table I gives a description of the tubes studied and the measured transmission. Tube B1 had excellent transmission before and after the drilling of electrode holes from the side. By slightly misaligning the tube with respect to the input beam, we excited higher order modes. The transmission was again >99%, thus indicating that the waveguide losses must be quite small as expected from the theory[1] ($\alpha_{theo} = 4.3 \times 10^{-5}$ cm). Although it is difficult to draw direct conclusions from such data, some recommendations can be made that will facilitate laser performance. Transmission measurements must be made on all tubes to ensure cleanliness and straightness of the bore and to reduce the waveguide transmission. If, after the fabrication procedures are completed, good transmission (>99%) is measured, the performance of the laser should not be affected by waveguide losses.

TABLE I

Experimental Tubes and Measured Transmission

Tube	Description	% Transmission
B1a	8.5 cm, no electrodes	>99%
B1b	B1a, with 4 electrodes	>99%
B2	5 cm with 6 electrodes	96%
B3	8.6 cm, with 6 electrodes	97%
B4	1.4 cm, no electrodes	>99%

T1055

c. Rough Wall Waveguide Measurements – To determine directly the dependence of waveguide resonator losses on wall roughness a simple one-dimensional structure was used. Two pyrex glass plates (3 cm x 9 cm x 0.5 cm) were spaced 1/2 mm apart, thus defining a one dimensional waveguide structure. One of the glass plates was roughened by sandblasting. The surface roughness was measured with a Dektak profiler. From the measurement of transmission and using an assumed coupling figure of 95% for gaussian to TM conversion, an absolute α for both smooth and roughened waveguides was obtained.

Our previously derived expressions for the transmission of a roughened waveguide may be modified to describe the case where only one surface is roughened, giving

$$\ell n\, T = \frac{L}{2a \cot \phi}\, \ell n\, rr'$$

where T is the transmission, a = 0.5 mm is the width of the guide, and r and r' are the reflectivities (at angle ϕ) for the smooth and roughened surfaces, respectively. Measured values of guide-transmission (as well as αL, r', and r'/r) are given in Table II. For the smooth surface, we have r' = r.

TABLE II

Transmission, Loss and Reflectivities for Three Structures

	T	αL	r'	r'/r
"Smooth"	0.805	0.220 cm^{-1}	0.942	1.0
SB 2	0.784	0.255	0.927	0.984
SB 5	0.708	0.35	0.876	0.930

According to Beckmann's theory for a normally distributed surface,

$$r'/r = e^{-\left(\frac{4\pi \sin \phi}{\lambda}\right)^2}$$

This allows us to calculate the rms roughness σ_{calc} from the measured values of r'/r and compare them with values of σ from Dektak measurements. We compare the calculated and measured values of σ for SB2 and SB5 in the following table.

	σ_{calc}	σ_{meas}
SB2	5 μm	8 μm
SB5	11	20

These results show that the calculated numbers are smaller than the measured values. This may be due to shadowing effects ($\sigma > \lambda$), which are not considered in Beckmann's analysis, or to inaccuracies in the determination of σ_{meas} from the Dektak plots.

However, the most important point established in this experiment is that SB2, which has a measured value of $\sigma = 8$ μm, still transmits 97.5% as much as the smooth walled waveguide. This 8 μm roughness is an order of magnitude larger than the measured roughness of the worst pyrex, quartz or even BeO waveguide candidates one might choose to implement in a laser. Here we have supporting experimental evidence for the contention that the wall roughness in the laser structures presently being made of BeO is of little consequence in determining laser performance.

III. CONCLUSIONS AND FUTURE PLANS

As we have shown in the previous sections, the tuning range of our present devices is limited to 1200 MHz. With improvements in diffraction gratings and optimization of tube cross section, we expect the laser tunability to be increased to 1.5 GHz. In order to achieve the goals of the present program, however, it will be necessary to improve the loss characteristics of the hollow waveguide as well as reducing its diameter.

In the previous section it was shown that the most important mechanisms for waveguide loss are likely to be mechanical imperfections or a lack of straightness of the laser bore. It is unlikely that straighter drilled holes can be fabricated, especially if we desire to simultaneously decrease bore diameter. In order to insure adequate tolerance on both the surface finish and bore straightness at smaller bore diameters, future tubes will be fabricated from square bores, using the technique described in Section II.

Another limitation on the measured tuning range has been the quality of the optical components. The diffraction grating has 3% loss and the output mirror (when used) presents a 4% loss (per round trip). Attempts to improve the efficiency of the grating have been described earlier in this report and are being pursued. The 4% loss from the output mirror (3% output, 1% dissipation) is also excessive. Dielectric mirrors from commercial vendors have proven to be of questionable reliability. We have found it important to carefully check reflectivity as well as transmission on purchased mirrors and we find the mirror loss is typically 0.5 to 1.0%. Laser heterodyne measurements have revealed that a mechanical resonance at ~2.2 kHz is presently limiting our short term frequency stability to ~100 kHz. A redesign of the mirror and bimorph holders should improve the situation.

In conclusion, preliminary experiments have proven that it is feasible to employ the proposed multiple electrode geometry and that a diffraction grating may be effectively used in a waveguide laser.

Hardware has been developed which has enabled us to demonstrate a CO_2 laser electronically tunable over 1200 MHz with less than 20 V of drive to the tuning element. A comprehensive study of loss mechanisms in hollow waveguides has been performed which shows that the most likely source of loss is lack of straightness rather than surface finish, as was previously assumed. Optimization of the bore diameter and improvement in the quality of the optical component should result in a tunable CO_2 laser capable of greater than 1.5 GHz of tuning.

REFERENCES

1. R. L. Abrams and W. B. Bridges, IEEE J. Quantum Electron., QE-9, 940 (September 1973).

2. E. A. J. Marcatili and R. A. Schmeltzer, Bell Syst. Tech. J. 43, 1783 (July 1964).

3. J. J. Degnan, J. Appl. Phys. (to be published).

4. P. Beckmann, The Scattering of Electromagnetic Waves from Rough Surfaces (Macmillan, New York, 1963), Part I.

5. E. Loh, Phys. Rev. 166, 673 (February 1968).

6. D. H. Hensler, Appl. Optics 11, 2522 (November 1973).

7. R. L. Abrams, IEEE J. Quantum Electron., QE-8, 838 (November 1973).

8. D. Marcuse, IEEE J. Quantum Electron., QE-8, 661 (July 1973).